

## RESEARCH ARTICLE

# Robust offset-free nonlinear model predictive control for systems learned by neural nonlinear autoregressive exogenous models<sup>†</sup>

Jing Xie | Fabio Bonassi | Marcello Farina | Riccardo Scattolini

Dipartimento di Elettronica,  
Informazione e Bioingegneria,  
Politecnico di Milano, Milano, Italy

**Correspondence**

Jing Xie, Dipartimento di Elettronica,  
Informazione e Bioingegneria, Politecnico di  
Milano, Via Ponzio 34/5, 20133, Milano,  
Italy.  
Email: jing.xie@polimi.it

**Funding Information**

This research was supported by the  
European Union's Horizon 2020 research  
and innovation programme under the Marie  
Skłodowska-Curie grant agreement  
No. 953348

**Abstract**

This paper presents a robust Model Predictive Control (MPC) scheme that provides offset-free setpoint tracking for systems described by Neural Nonlinear AutoRegressive eXogenous (NNARX) models. The NNARX model learns the dynamics of the plant from input-output data, and during the training the Incremental Input-to-State Stability ( $\delta$ ISS) property is forced to guarantee stability. The trained NNARX model is then augmented with an explicit integral action on the output tracking error, which allows the control scheme to enjoy offset-free tracking ability. A tube-based MPC is finally designed, leveraging the unique structure of the model, to ensure robust stability and robust asymptotic zero error regulation for constant reference signals in the presence of model-plant mismatch or unknown disturbances. Numerical simulations on a water heating system show the effectiveness of the proposed control algorithm.

**KEYWORDS:**

nonlinear model predictive control, offset-free tracking, neural networks, robust control, learning-based control

## 1 | INTRODUCTION

Learning algorithms for model identification and control design are increasingly popular in the control community.<sup>1,2</sup> Among the main approaches developed so far, we here recall Gaussian processes,<sup>3</sup> set membership identification algorithms,<sup>4</sup> and Bayesian identification,<sup>5</sup> where large and informative data-sets are utilized to extract important information on the characteristics of the system under control. In this framework, Recurrent Neural Networks (RNN) are also widely used, see References 6 and 7, due to their ability to describe strongly nonlinear dynamics. In addition, recently many efforts have been put into the analysis of stability properties of various RNN structures such as Gated Recurrent Units (GRU),<sup>8</sup> Short Term Memory networks (LSTM),<sup>9</sup> Echo State Networks (ESN),<sup>10</sup> and Neural Nonlinear AutoRegressive eXogenous models (NNARX).<sup>11</sup> In these works, sufficient conditions for Input-to-State Stability (ISS) and Incremental Input-to-State Stability of the adopted RNN model ( $\delta$ ISS) have been derived. Notably, these conditions can be enforced during the training phase of RNNs, and allow to obtain theoretically sound methods for the design of Model Predictive Control strategies for systems described with RNN models, see References 9 and 10. An overview on the advantages of RNN with stability properties is reported in Reference 12, together with an in-depth discussion on the many issues to be considered when using RNN for control design, such as verifiability, interpretability, and lifelong learning.

A further step towards the application of MPC with RNN models concerns the development of control schemes guaranteeing the asymptotic zero error regulation for constant exogenous signals also in presence of modeling errors, plant's changes, or additive disturbances. To this end, several offset-free tracking MPC algorithms have been proposed both for linear and nonlinear

<sup>†</sup>This work has been submitted to the Wiley for possible publication. Copyright may be transferred without notice, after which this version may no longer be accessible.

plant models. In Reference 13, the model is augmented with an integrator on the output tracking error, and an observer is designed to reconstruct the state of the system. In this solution, offset-free is achieved without defining and estimating any disturbance. This approach is adopted also in Reference 14, where an offset-free MPC control scheme is designed for systems learned by GRU networks. A second, very popular approach is proposed in Reference 15, where the system is augmented with a (fictitious) disturbance model. The estimation of this disturbance is then used to compute the steady-state values of the system's states and inputs which guarantee zero error regulation also in case of plant-model mismatches.

Regardless of the problem of asymptotic zero error regulation, model uncertainties and/or perturbations can cause the violation of state and input constraints. In addition, nominal stability can be lost, which can pose huge risks for safety-critical systems. In this context, several robust MPC algorithms have been proposed, such as min-max MPC,<sup>16</sup> where the optimal control sequence is computed by minimizing the cost function in the worst case scenario. However, this method results in a computationally intractable optimization problem, so that an effective alternative is the popular tube-based approach,<sup>17,18</sup> mainly developed for linear systems, but also extended to the nonlinear case.

In this paper, we propose a solution to the *robust zero error regulation* problem for systems described by Neural NARX models. The choice of NNARX is motivated by their simple structure and easy training. In addition, the state of NNARXs consists only of past input-output data, so that a state observer is not needed in the implementation of the MPC algorithm. Along the lines of References 13 and 14, we propose to augment the control structure with two elements: (i) an integrator on the output tracking error, to achieve asymptotic offset-free tracking; (ii) a derivative action on the MPC output, useful to apply almost standard stability results for nominal and robust "tube-based" MPC. Some preliminary results, obtained by considering only the nominal case, have been reported in Reference 19.

The proposed approach has been tested on the model of a water heating benchmark system. The goals are twofold. First, in the nominal case the closed-loop performances of the proposed MPC are compared to those achieved by the strategy proposed in Reference 15. The simulation results show remarkable performance of the proposed approach even in presence of significant disturbances. Second, the perturbed case in which model mismatch is present is considered and the performances of the proposed tube-based MPC are illustrated.

The paper is structured as follows. In Section 2 the NNARX nominal model and the perturbed system are introduced. In Section 3 the proposed robust control framework is described in detail. Then, in Section 4 the proposed control architecture is tested on a simulated water heating benchmark system. Lastly, some conclusions are drawn in Section 5.

## 1.1 | Notation

The following notation is adopted in this paper. Let  $R$  denote the field of real numbers,  $R^n$  the  $n$ -dimensional Euclidean space. Given a vector  $v$ ,  $v'$  is its transpose,  $\|v\|_p$  its  $p$ -norm and  $\|v\|_\infty$  its maximum norm. In addition, given a matrix  $Q$ , we denote  $\|v\|_Q^2 := v'Qv$ . Sequences of vectors are indicated by bold-face fonts, i.e.,  $\mathbf{v}_k = \{v_0, \dots, v_k\}$ . Given two sets  $\mathcal{A}$  and  $\mathcal{B}$ ,  $\mathcal{A} \oplus \mathcal{B} := \{a + b | a \in \mathcal{A}, b \in \mathcal{B}\}$  denotes the Minkowski set addition and  $\mathcal{A} \ominus \mathcal{B} := \{a | a \oplus \mathcal{B} \subseteq \mathcal{A}\}$  the Pontryagin set subtraction.

## 2 | PROBLEM STATEMENT AND NNARX MODEL

The robust tracking problem we want to solve can be described as follows. Consider a general dynamical system

$$y = S(u), \quad (1)$$

with input  $u \in \mathcal{U} \subset R^m$  and output  $y \in \mathcal{Y} \subset R^p$ , where  $\mathcal{U}$  and  $\mathcal{Y}$  are closed sets. For simplicity, in the following it is assumed that the number of outputs  $p$  equals the number of inputs  $m$ , but the proposed approach can be easily extended to the case  $m \geq p$ .

Assume that the nominal model of the plant is described by

$$\bar{y} = \bar{S}(u), \quad (2)$$

where output  $\bar{y} \in \mathcal{Y} \subset R^p$ . Let a suitable representation of the modeling error (to be specified later) be known. The aim of this work is to design for  $S$ , based on  $\bar{S}$ , an MPC control law guaranteeing closed-loop stability and robust asymptotic zero error regulation for constant reference signals  $y^o \in \mathcal{Y} \subset R^p$ .

In this paper, the above-mentioned problem is tackled in three steps:

- i. definition of the nominal NNARX model of  $\bar{S}$  and of the modeling error;

- ii. definition of a control structure with guaranteed robust asymptotic zero error regulation also in case of model mismatch, provided that nominal stability is maintained;
- iii. definition of a robust MPC algorithm guaranteeing constraints' satisfaction and stability results also in the perturbed case  $\bar{S} \neq S$ .

## 2.1 | Neural NARX nominal model

The nominal model  $\bar{S}$  is assumed to be described by a NNARX structure, see Reference 11, where the output  $\bar{y}_{k+1}$  is computed as a regression over past  $N$  input and output samples as well as current input  $u_k$ :

$$\bar{y}_{k+1} = \eta(\bar{y}_k, \bar{y}_{k-1}, \dots, \bar{y}_{k-N+1}, u_k, u_{k-1}, \dots, u_{k-N}; \Phi), \quad (3)$$

where  $\eta$  denotes the regression function and  $\Phi$  is the set of model parameters.

Model (3) can be given a discrete state space form by defining the state vector containing the past information as

$$z_{i,k} = \begin{bmatrix} \bar{y}_{k-N+i} \\ u_{k-N-1+i} \end{bmatrix} \quad (4)$$

with  $i \in \{1, \dots, N\}$ . The model (3) is equivalent to

$$\begin{cases} z_{1,k+1} = z_{2,k} \\ \vdots \\ z_{N-1,k+1} = z_{N,k} \\ z_{N,k+1} = \begin{bmatrix} \eta(z_{1,k}, z_{2,k}, \dots, z_{N,k}, u_k; \Phi) \\ u_k \end{bmatrix} \\ \bar{y}_k = [I \quad 0] z_{N,k} \end{cases} \quad (5)$$

Define now the nominal state vector  $\bar{x}_k = [z'_{1,k}, \dots, z'_{N,k}]' \in R^n$ , where  $n = N(m+p)$ . Note that, in view of the previous definitions, it holds that  $\bar{x} \in \bar{\mathcal{X}}$ , where  $\bar{\mathcal{X}}$  can be easily expressed in terms of  $\mathcal{U}$ ,  $\mathcal{Y}$ .

Model (5) can be compactly reformulated as

$$\begin{cases} \bar{x}_{k+1} = A\bar{x}_k + B_u u_k + B_x \eta(\bar{x}_k, u_k) \\ \bar{y}_k = C\bar{x}_k \end{cases} \quad (6a)$$

where  $A$ ,  $B_u$ ,  $B_x$ , and  $C$  are:

$$A = \begin{bmatrix} 0 & I & 0 & \dots & 0 \\ 0 & 0 & I & \dots & 0 \\ \vdots & & & \ddots & \vdots \\ 0 & 0 & 0 & \dots & I \\ 0 & 0 & 0 & \dots & 0 \end{bmatrix}, \quad B_u = \begin{bmatrix} 0 \\ 0 \\ \vdots \\ 0 \\ \tilde{B}_u \end{bmatrix}, \quad B_x = \begin{bmatrix} 0 \\ 0 \\ \vdots \\ 0 \\ \tilde{B}_x \end{bmatrix}, \quad C = [0 \quad \dots \quad 0 \quad \tilde{C}]. \quad (6b)$$

$0$  and  $I$  are null and identity matrices of proper dimensions, and the sub-matrices  $\tilde{B}_u$ ,  $\tilde{B}_x$ , and  $\tilde{C}$  are defined as

$$\tilde{B}_u = \begin{bmatrix} 0 \\ I \end{bmatrix}, \quad \tilde{B}_x = \begin{bmatrix} I \\ 0 \end{bmatrix}, \quad \tilde{C} = [I \quad 0]. \quad (6c)$$

The regression function  $\eta$  in (6) is a Feed-Forward Neural Network (FFNN) consisting of  $M$  layers of neurons. Each layer is a linear combination of its inputs, coupled with a nonlinear activation function. A compact formulation of  $\eta$  is

$$\eta(x_k, u_k) = U_0 \eta_M (\eta_{M-1} (\dots \eta_1 (x_k, u_k), u_k), u_k) + b_0 \quad (7)$$

where  $\eta_t$  with  $t \in \{1, \dots, M\}$  is the nonlinear relation in  $t$ -th layer, which can be denoted as

$$\eta_t(\eta_{t-1}, u_k) = \sigma_t(W_t u_k + U_t \eta_{t-1} + b_t). \quad (8)$$

The activation function  $\sigma_t$  is selected to be Lipschitz-continuous with Lipschitz constant  $L_{\sigma_t}$  and zero-centered, i.e.,  $\sigma_t(0) = 0$ . The matrices  $W_t$ ,  $U_t$  and  $b_t$  are the weights of each layer, which are training parameters of the network  $\Phi =$

$\{U_0, b_0, \{U_t, W_t, b_t\}_{t=1, \dots, M}\}$ . Omitting  $\Phi$  for compactness, the NNARX model (6) can be written as

$$\Sigma : \begin{cases} \bar{x}_{k+1} = f(\bar{x}_k, u_k) \\ \bar{y}_k = C\bar{x}_k \end{cases}. \quad (9)$$

In the training phase, the parameters  $\Phi$  are estimated from data by minimizing a certain cost function under constraints guaranteeing stability properties, i.e., ISS and  $\delta$ ISS, see Reference 11. This is of particular interest under the implicit assumption that the system displays suitable stability-like properties. The definition of  $\delta$ ISS for the generic nonlinear system (9) is reported below.

**Definition 1** ( $\delta$ ISS). System (9) is  $\delta$ ISS if there exist functions  $\beta \in \mathcal{KL}$  and  $\gamma \in \mathcal{K}_\infty$  such that, for any pair of initial states  $\bar{x}_{a,0}$  and  $\bar{x}_{b,0}$ , and any pair of input sequences  $\mathbf{u}_a$  and  $\mathbf{u}_b$ , where all the elements in both sequences satisfy  $u_{a,k} \in \mathcal{U}$  and  $u_{b,k} \in \mathcal{U}$ , such that

$$\|\bar{x}_{a,k} - \bar{x}_{b,k}\|_2 \leq \beta(\|\bar{x}_{a,0} - \bar{x}_{b,0}\|_2, k) + \gamma(\|\mathbf{u}_a - \mathbf{u}_b\|_{2,\infty}) \quad (10)$$

for any  $k \geq 0$ , where  $\bar{x}_{*,k}$  denotes the state trajectory of the system initialized in  $\bar{x}_{*,0}$  and fed by the sequence  $\mathbf{u}_*$ .

Motivated by the existing literature concerning the training of  $\delta$ ISS networks,<sup>11,12</sup> the following Assumption is now introduced.

**Assumption 1.** The NNARX model (9) is  $\delta$ ISS.

## 2.2 | Perturbed Model

Let the real system dynamics be described by

$$\begin{cases} x_{k+1} = Ax_k + B_u u_k + B_x \eta(x_k, u_k) + B_x \delta(x_k, u_k) \\ y_k = Cx_k \end{cases} \quad (11)$$

where the state  $x_k$  has the same structure of  $\bar{x}_k$ . Note that the dependence of  $\eta$  upon its parameters  $\Phi$  has been removed for clarity, and that  $B_x \delta(x_k, u_k)$  represents an unknown uncertainty affecting the component of  $x_k$  that corresponds to  $y_k$ . Then, defining the state error  $e_k = x_k - \bar{x}_k$  as the deviation between the real state  $x_k$  and the nominal one  $\bar{x}_k$ , from (6) and (11) it can be obtained that

$$e_{k+1} = Ae_k + \underbrace{B_x [\eta(x_k, u_k) - \eta(\bar{x}_k, u_k) + \delta(x_k, u_k)]}_{w_k}, \quad (12)$$

which consists of a linear component,  $Ae_k$ , and a nonlinear one produced by the model mismatch,  $\eta(x_k, u_k) - \eta(\bar{x}_k, u_k)$ , and by the uncertainty  $\delta(x_k, u_k)$ . Letting

$$w_k = B_x [\eta(x_k, u_k) - \eta(\bar{x}_k, u_k) + \delta(x_k, u_k)]$$

be the equivalent disturbance, we assume that  $w_k \in \mathcal{W}$  for all  $k$ , where  $\mathcal{W}$  is a closed and compact set which depends on  $\mathcal{X}$ ,  $\mathcal{U}$ .

**Assumption 2.** The disturbance  $w$  is bounded in a compact set  $\mathcal{W}$  of radius  $\check{w}$ , i.e. for any  $k$

$$w_k \in \mathcal{W} = \{w \in \mathbb{R}^n : \|w\|_2 \leq \check{w}\} \quad (13)$$

In the spirit of the data-driven control approach taken in this paper, the value of  $\check{w}$  can be estimated from data. In particular, due to the structure of matrix  $B_x$ , see (6), the disturbance  $w_k$  only affects the entry of  $x_{k+1}$  associated to  $y_{k+1}$ . This property can be exploited when constructing a polyhedron representation of the set  $\mathcal{W}$ .

## 3 | CONTROLLER DESIGN

As previously stated, the goal of this paper is to design a control system such that the controlled output tracks a given constant reference signal  $y^o$  in a robust way, i.e.

$$\varepsilon_k = y^o - y_k \xrightarrow[k \rightarrow \infty]{} 0. \quad (14)$$

also in presence of model mismatch.

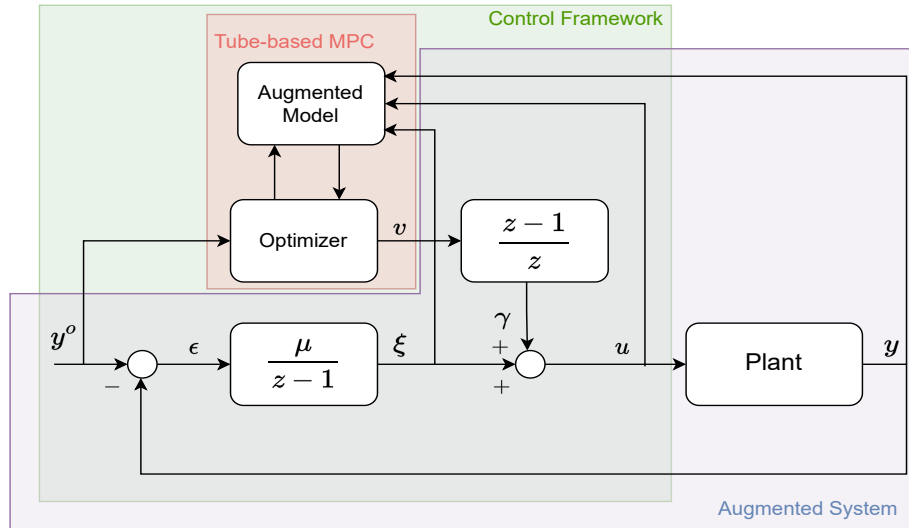


**Figure 1** Schematic of the proposed control framework

### 3.1 | Tracking in the nominal case

To introduce the proposed control structure, we first consider the control design in the nominal case. To this end, let  $(\bar{x}(y^o), \bar{u}(y^o))$  be a feasible equilibrium, meaning that  $\bar{x}(y^o) \in \mathcal{X}$  and  $\bar{u}(y^o) \in \mathcal{U}$  satisfy

$$\begin{cases} \bar{x}(y^o) = f(\bar{x}(y^o), \bar{u}(y^o)) \\ y^o = C\bar{x}(y^o) \end{cases} \quad (15)$$

Then, consider the linearization of the system (9) around such equilibrium, defined by the matrices

$$A_\delta = \left. \frac{\partial f(x, u)}{\partial x} \right|_{(\bar{x}(y^o), \bar{u}(y^o))}, \quad B_\delta = \left. \frac{\partial f(x, u)}{\partial u} \right|_{(\bar{x}(y^o), \bar{u}(y^o))} \quad (16)$$

The following result specifies the stability properties of the linearized model.

**Proposition 1.** Consider a nonlinear system in the form (9). Assume that it is  $\delta$ ISS in the sense specified by Definition 1, and that the function  $\beta$  admits an exponential form, i.e. that there exist constants  $\rho > 0$  and  $\lambda \in (0, 1)$  such that  $\beta(\|\bar{x}_{a,0} - \bar{x}_{b,0}\|_2, k) \leq \rho \|\bar{x}_{a,0} - \bar{x}_{b,0}\|_2 \lambda^k$ . In addition, assume that the gradient of  $f(x, \bar{u}(y^o))$  with respect to  $x$  is Lipschitz continuous with Lipschitz constant  $L_1$ . Then, for each feasible equilibrium  $(\bar{x}(y^o), \bar{u}(y^o))$  satisfying (16), the matrix  $A_\delta$  is Schur stable.

*Proof.* See the Appendix. □

Note that the exponential form of function  $\beta$  is indeed enjoyed by  $\delta$ ISS RNNs, see References 8 and 9, and specifically<sup>11</sup> for NNARXs. The matrix  $A_\delta$  of the linearized system defined in (16) is therefore Schur stable. In addition, the following Assumption on the linearized system matrices is introduced.

**Assumption 3.** The tuple  $(A_\delta, B_\delta, C)$  is reachable, observable, and does not have invariant zeros equal to 1.

Under Assumption 3 and in light of Theorem 1 in Reference 20, one can guarantee the existence of an open neighborhood of  $y^o$ , denoted by  $\Gamma(y^o) \subseteq \mathcal{R}^p$ , where, for any  $\tilde{y} \in \Gamma(y^o)$ , there exists an equilibrium  $(\tilde{x}(\tilde{y}), \tilde{u}(\tilde{y}))$  satisfying the state and input constraints and such that

$$\begin{cases} \tilde{x}(\tilde{y}) = f(\tilde{x}(\tilde{y}), \tilde{u}(\tilde{y})) \\ \tilde{y} = C\tilde{x}(\tilde{y}) \end{cases} \quad (17)$$

This local result allows to conclude that it is possible to move the output reference signal in a neighborhood  $\Gamma(y^o)$  of  $y^o$  and still guarantee that a feasible solution to the tracking problem exists.

### 3.2 | Control scheme

The control scheme we propose is shown in Figure 1. The regulator is made by three main blocks: an integrator of the output tracking error, an MPC algorithm, and a derivative action. Its rationale is the following:

- The integrator acts on the output tracking error  $\varepsilon_k = y^o - y_k$ , so that, in light of the Internal Model Principle,<sup>21</sup> it is ensured that  $\varepsilon_k$  asymptotically converges to zero also in presence of modeling error or additive disturbances, provided that the closed-loop system remains asymptotically stable. The gain  $\mu$  of the integrator must be selected to guarantee stability properties. This choice is later discussed.
- The MPC algorithm provides improved performances in transient conditions and the fulfillment of input and output constrains, while at the steady state its action is null due to the derivative action acting on its output.
- The derivative action is required to achieve stability results for the overall system by means of a standard zero terminal constraint formulation of MPC.

More formally, the integral block is described by

$$\xi_{k+1} = \xi_k + \mu(y^o - \bar{y}_k), \quad (18)$$

with  $\xi \in R^m$ ,  $\mu \in R^{m,m}$ , while the derivative action is

$$\begin{cases} \theta_{k+1} = v_k \\ \gamma_k = v_k - \theta_k \end{cases}, \quad (19)$$

where  $v \in R^m$  is the output of the MPC regulator.

According to Figure 1, the resulting control action  $u_k$  is given by

$$u_k = \xi_k + \gamma_k. \quad (20)$$

Note that, as already discussed, at steady state  $\gamma = 0$  the control variable  $u$  is uniquely defined by the integral action.

In view of the previous definitions, the overall system to be considered in the design of the MPC algorithm in nominal conditions is obtained from (9), (18), (19), (20), and takes the form

$$\begin{cases} \bar{x}_{k+1} = f(\bar{x}_k, u_k) \\ \xi_{k+1} = \xi_k + \mu(y^o - \bar{y}_k) \\ \theta_{k+1} = v_k \\ \gamma_k = v_k - \theta_k \\ u_k = \xi_k + \gamma_k \\ \bar{y}_k = C\bar{x}_k \end{cases}, \quad (21)$$

Defining the augmented state  $\bar{\chi}_k = [\bar{x}_k', \xi_k', \theta_k']'$  and the augmented output  $\bar{\zeta}_k = [\bar{y}_k', u_k']'$ , (21) can be rewritten in the general form

$$\bar{\Sigma}_a : \begin{cases} \bar{\chi}_{k+1} = f_a(\bar{\chi}_k, v_k, y^o) \\ \bar{\zeta}_k = g_a(\bar{\chi}_k, v_k) \end{cases}, \quad (22)$$

with suitable functions  $f_a, g_a$ .

Now denote by  $(\bar{\chi}(y^o), \bar{v}(y^o), \bar{\zeta}(y^o))$  the (feasible) state, input, and output equilibrium values corresponding to the output  $\bar{y} = y^o$  of the enlarged system  $\bar{\Sigma}_a$ . Note that at equilibrium  $\bar{\gamma} = 0$ ,  $\bar{\xi} = \bar{u}$ , and  $\bar{v}$  can take any value. The following proposition can thus be stated, providing guidelines for the design of the integrator gain  $\mu$ .

**Proposition 2.** Under Assumption 3 and Proposition 1, there exists  $\check{\mu} > 0$  such that, for any  $\hat{\mu} \in (0, \check{\mu})$ , the integrator gain

$$\mu = \hat{\mu} [C(I - A_\delta)^{-1} B_\delta]^{-1} \quad (23)$$

ensures that the enlarged system (22), linearized around  $(\bar{\chi}(y^o), \bar{v}(y^o), \bar{\zeta}(y^o))$ , is asymptotically stable

*Proof.* In light of Proposition 1, the matrix  $A_\delta$  is Schur stable. Then, under Assumption 3, the results in Reference 22 prove the Proposition.  $\square$

Note that Proposition 2 not only guarantees the existence of a stabilizing integrator gain, but also shows how to compute such gain. In practice,  $\mu$  is computed according to (23) for increasing values of  $\hat{\mu}$ , and the asymptotic stability of the linearization of  $\bar{\Sigma}_a$  is assessed.

### 3.3 | Nominal MPC design

A nominal stabilizing nonlinear MPC law is now designed for the nominal augmented system model. The constrained optimization problem to be solved at any time instant  $k$  is

$$\min_{v_{0|k}, \dots, v_{N_p-1|k}} \sum_{i=0}^{N_p} \left[ \left\| \bar{x}_{i|k} - \bar{x}(y^o) \right\|_Q^2 + \left\| \bar{\zeta}_{i|k} - \bar{\zeta}(y^o) \right\|_R^2 \right] \quad (24a)$$

$$\text{s.t. } \forall i \in \{0, \dots, N_p - 1\}$$

$$\bar{x}_{0|k} = \bar{x}_k \quad (24b)$$

$$\bar{x}_{i+1|k} = f_a(\bar{x}_{i|k}, v_{i|k}, y^o) \quad (24c)$$

$$\bar{\zeta}_{i|k} = g_a(\bar{x}_{i|k}, v_{i|k}) \quad (24d)$$

$$S_x \bar{x}_{i|k} \in \mathcal{X} \quad (24e)$$

$$S_u \bar{\zeta}_{i|k} \in \mathcal{U} \quad (24f)$$

$$\bar{x}_{N_p|k} = \bar{x}(y^o) \quad (24g)$$

In MPC cost function (24a),  $N_p$  is the prediction horizon, and the weight matrix  $Q = \text{diag}(Q_x, Q_\xi, Q_\theta)$ , where  $\text{diag}(\cdot)$  denotes the block-diagonal operator, penalizes the displacement of the state vector  $\bar{x}$  from its equilibrium. The weight matrix  $R$  is defined as  $\text{diag}(R_y, R_u)$ , where  $R_y$  and  $R_u$  penalize the output error and the control effort, respectively.

The augmented nominal model  $\bar{\Sigma}_a$ , defined in (22), is used as predictive model, see (24c) and (24d), and it is initialized with known current values, see (24b). Moreover, (24e) and (24f) enforce the saturation constraints on  $\bar{x}_{i|k}$  and  $u_{i|k}$ , where the matrix  $S_x$  selects  $\bar{x}_{i|k}$  from the state vector  $\bar{\xi}_{i|k}$  and  $S_u$  selects  $u_{i|k}$  from the output vector  $\bar{\zeta}_{i|k}$ . Finally the terminal equality constraint (24g) is introduced to provide stability.

The solution to problem (24) at the time instant  $k$  yields the optimal control sequence  $v_k^* = \{v_{0|k}^*, v_{1|k}^*, \dots, v_{N_p-1|k}^*\}$ . Then, according to the Receding Horizon approach, only the first element in the sequence is applied and the implicit MPC control law reads

$$v_k = \kappa_k(\bar{x}_k) = v_{0|k}^*. \quad (25)$$

The procedure is repeated at the successive time step  $k + 1$ , based on the measured state  $\bar{x}_{k+1} = [\bar{x}'_{k+1}, \xi'_{k+1}, \theta'_{k+1}]'$ , which leads to a state-feedback control law.

Note that the formulation (24) is a standard zero terminal constraint MPC, and nominal recursive feasibility and closed-loop stability can be guaranteed with standard arguments, see Reference 23.

### 3.4 | Robust MPC design

The robust MPC controller is designed according to the popular “tube-based” approach, see Reference 17. To this end, to compute for the perturbed error system (12) a Robust Positively Invariant (RPI) set  $\Omega_x$  such that, if the real system state  $x_k \in \bar{x}_k \oplus \Omega_x$ , then  $x_{k+i} \in \bar{x}_{k+i} \oplus \Omega_x$  for all  $i > 0$ , and for any admissible disturbance realization  $w_k \in \mathcal{W}, \dots, w_{k+i-1} \in \mathcal{W}$ .

In general, the analytical computation of  $\Omega_x$  is difficult, or even impossible, so that approximate solutions are often used. However, in our case the system matrix  $A$  in (6) is Schur stable and nilpotent, so that, according to Reference 24, the RPI is given by

$$\Omega_x = \sum_{j=0}^{N-1} A^j \mathcal{W}, \quad (26)$$

where  $\sum_j$  is here used to denote the Minkowski set addition and  $N$  is the number of past input-output data of the NNARX model. Therefore, owing to the specific structure of NNARX models, one of the most critical issues in the design of robust “tube-based” MPC laws is easily overcome.

In view of the previous considerations, the adopted formulation for nonlinear robust MPC reads as

$$\min_{\substack{v_{0|k}, \dots, v_{N_p-1|k} \\ \bar{x}_{0|k}}} \sum_{i=0}^{N_p} \left[ \left\| \bar{x}_{i|k} - \bar{x}(y^o) \right\|_Q^2 + \left\| \bar{\zeta}_{i|k} - \bar{\zeta}(y^o) \right\|_R^2 \right] \quad (27a)$$

$$\text{s.t. } \forall i \in \{0, \dots, N_p - 1\}$$

$$S_x \bar{x}_{0|k} \in \{\bar{x}_k\} \oplus \Omega_x \quad (27b)$$

$$S_\xi \bar{x}_{0|k} = \xi_k \quad (27c)$$

$$S_\theta \bar{x}_{0|k} = v_k \quad (27d)$$

$$\bar{x}_{i+1|k} = f_a(\bar{x}_{i|k}, v_{i|k}, y^o) \quad (27e)$$

$$\bar{\zeta}_{i|k} = g_a(\bar{x}_{i|k}, v_{i|k}) \quad (27f)$$

$$S_x \bar{x}_{i|k} \in \mathcal{X} \ominus \Omega_x \quad (27g)$$

$$S_u \bar{\zeta}_{i|k} \in \mathcal{U} \quad (27h)$$

$$\bar{x}_{N_p|k} = \bar{x}(y^o) \quad (27i)$$

The cost function (27a) adopted is the same as in the nominal MPC, see (24a), and it penalizes the distances of the augmented system's state and output from their targets. The main difference lies, however, in the initialization of the component  $\bar{x}_{0|k}$  of the augmented state vector. Rather than fixing it to the known measured value  $\bar{x}_k$ , it is considered as a free optimization variable lying in the RPI set  $\bar{x}_k \oplus \Omega_x$ , see (27b). Note that  $S_x$ ,  $S_\xi$  and  $S_\theta$  denote the selection matrices that extract  $\bar{x}_{i|k}$ ,  $\bar{\zeta}_{i|k}$ , and  $\bar{\theta}_{i|k}$  from  $\bar{x}_{i|k}$ , respectively.

The nominal augmented model  $\bar{\Sigma}_a$  is then used as predictive model, see (27e) and (27f). To ensure the robust constraint satisfaction, the constraint on state  $\bar{x}_{i|k}$  is tightened, see (27g). The input variable  $u_{i|k}$  is constrained to fulfill the actuator constraints, see (27h).

Solving the optimization problem (27), the optimal control sequence  $\mathbf{v}_k^* = \{v_{0|k}^*, \dots, v_{N_p-1|k}^*\}$  is retrieved. Then, according to the Receding Horizon principle, the first optimal control action  $v_{0|k}^*$  is applied, and at the following time-step the entire procedure is repeated. The corresponding implicit robust control law is denoted by

$$v_k = \kappa_k(\bar{x}_k) = v_{0|k}^* \quad (28)$$

Notably, such control law keeps the trajectory of the state of the perturbed system (11), i.e.  $x_k$ , in the robust control invariant set  $\Omega_x$  centered along the nominal state trajectory  $\bar{x}_k$ . This implies that the output  $y_k$  of the perturbed system is constrained in the set  $\Omega_y = C\Omega_x$  centered around the nominal output trajectory  $\bar{y}_k$ .

Lastly, we point out that the MPC law formulated in (27) follows from (24). The RPI set  $\Omega_x$  is robustly exponentially stable for the controlled uncertain system (11), see Reference 17. Recursive feasibility can also be guaranteed according to Proposition 3.14 in Reference 23.

## 4 | NUMERICAL EXAMPLE

### 4.1 | Benchmark system

A water-heating benchmark system depicted in Figure 2 is used to test the proposed control framework. The goal of the system is to regulate the temperature of the outlet water  $T$  to a desired value with the required flow rate. The inlet water flow rate is assumed to be the same as the outlet water flow rate  $w$ , keeping the water level in the tank constant.  $w_c$  denotes the inlet gas flow rate, which is burnt to heat the metal, and subsequently, heat the water in the tank.  $T_i$  and  $T_m$  denote the temperature of the inlet water and the metal respectively. The system dynamics read

$$\begin{cases} \dot{T} = \frac{1}{\rho_w A_t z_w} \left[ w (T_i - T) + \frac{k_{lm} A_t}{c_w} (T_m - T) \right] \\ \dot{T}_m = \frac{1}{M_m c_m} \left[ -k_{lm} A_t (T_m - T) + \sigma k_f w_c (T_f^4 - T_m^4) \right] \end{cases} \quad (29)$$

The model has one manipulable input  $u = w_c$ , one output  $y = T$  and two system states  $x = [T, T_m]^T$ . Both  $T_i$  and  $w$  in the system dynamics (29) can be treated as disturbances, i.e.,  $d = [T_i, w]^T$ . The nominal values of both disturbances are reported in

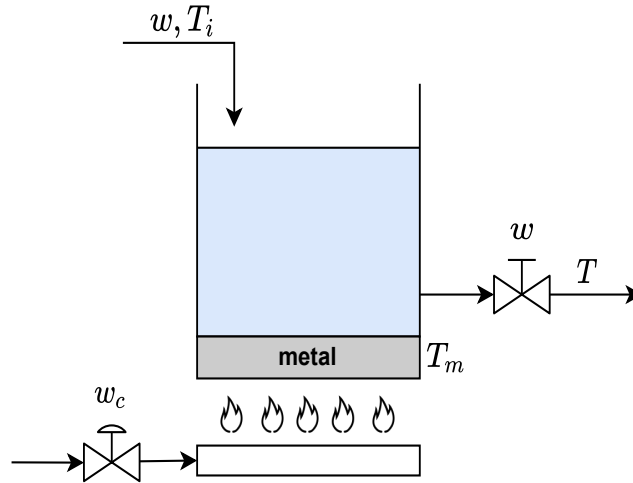


**Figure 2** Water-heating system illustration

**Table 1** Benchmark system parameters

| Parameter   | Description                     | Value                 | Units                     |
|-------------|---------------------------------|-----------------------|---------------------------|
| $A_t$       | Tank's cross-section            | $\frac{\pi}{4}$       | $m^2$                     |
| $\rho_w$    | Water's density                 | 997.8                 | $\frac{kg}{m^3}$          |
| $c_w$       | Water's specific heat           | 4180.0                | $\frac{kg \cdot K}{J}$    |
| $M_m$       | Metal plate's mass              | 617.32                | $kg$                      |
| $c_m$       | Metal's specific heat           | 481.0                 | $\frac{J}{kg \cdot K}$    |
| $\sigma$    | Radiation coefficient           | $5.67 \times 10^{-8}$ | $\frac{W}{m^2 \cdot K^4}$ |
| $k_{lm}$    | Heat exchange coefficient       | 3326.4                | $\frac{kg}{s^3 \cdot K}$  |
| $T_f$       | Flame's temperature             | 1200                  | $K$                       |
| $k_f$       | Heat exchange coefficient       | 8.0                   | $\frac{m^2 \cdot s}{kg}$  |
| $z_w$       | Water level                     | 2.0                   | $m$                       |
| $\bar{w}$   | Nominal water flow rate         | 1.0                   | $\frac{kg}{s}$            |
| $\bar{T}_i$ | Nominal inlet water temperature | 298                   | $K$                       |

Table 1, together with other parameters. Moreover, there is a constraint on the input,

$$w_c \in [0.05, 0.18]. \quad (30)$$

The benchmark system has been implemented in Simulink. The simulations have been carried out to collect the input-output data, which will be used to train Neural NARX model and test the proposed control algorithm.

## 4.2 | NNARX model training

To generate the dataset for training the Neural NARX model of the plant (29), the simulator has been fed with a Multilevel Pseudo-Random Signal (MPRS) to properly excite the system in the operating region (30). One input-output trajectory  $T_{exp}$ , with a total length of 2500 time steps, has been collected with sampling time  $\tau_s = 120s$ . According to the Truncated Back-Propagation Through Time (TBPTT) principle,<sup>25</sup>  $N_t = 120$  subsequences of length  $T_s^t = 400$  time steps, have been extracted from  $T_{exp}$ . We denote these sequences  $(\mathbf{u}^{(i)}, \mathbf{y}^{(i)})$  with  $i \in \mathcal{I}_t = \{1, \dots, N_t\}$ . The validation set and test set consist of  $N_v = 30$  and  $N_f = 1$  subsequences respectively, with length  $T_s = 1000$  time steps. Both sets are constructed by using completely independent

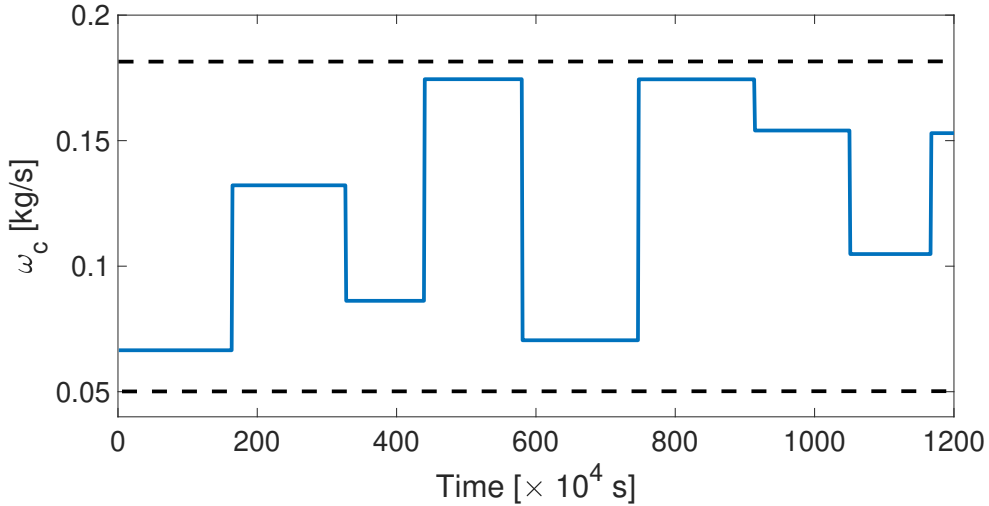


**Figure 3** Input sequence used for validation.

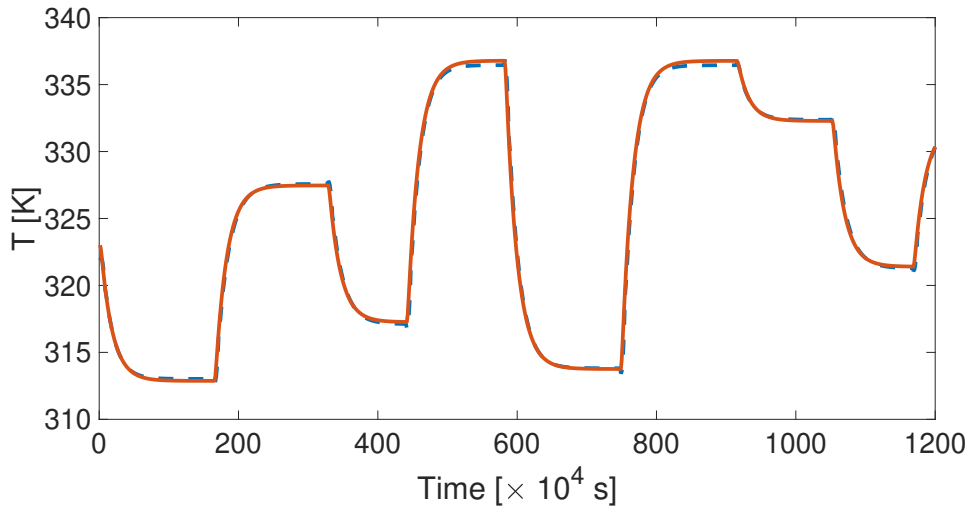


**Figure 4** Open-loop prediction (blue dashed line) versus ground truth (red continuous line).

simulation data. We denote validation and test set by the set of indices  $\mathcal{I}_v = \{N_t + 1, \dots, N_t + N_v\}$  and  $\mathcal{I}_f = \{N_t + N_v + 1, \dots, N_s\}$ , respectively, where  $N_s = N_t + N_v + N_f$ .

The training procedure has been carried out with PyTorch 1.9 and Python 3.9. The adopted Neural NARX model features a single-layer ( $M = 1$ ) FFNN with 30 neurons and activation function  $\sigma_t = \tanh$  in (8). The look-back horizon is  $N = 5$ . During the training procedure, the Mean Square Error (MSE) over the training set  $\mathcal{I}_t$  is minimized. A suitable regularization term is included in the cost function<sup>11</sup> so that Assumption 1 is satisfied. The training takes 1288 epochs until the modeling performance over the validation set  $\mathcal{I}_v$  saturates. Lastly, the trained Neural NARX has been tested on the independent test set  $\mathcal{I}_f$ . In Figure 3, the test input sequence  $\mathbf{u}^{(ts)}$  is shown. In Figure 4, the resulting output sequence  $\mathbf{y}^{(ts)} = \{y_0^{(ts)}, y_1^{(ts)}, \dots, y_{T_s}^{(ts)}\}$  of the Neural NARX model is compared to the ground truth sequence  $\bar{\mathbf{y}}^{(ts)} = \{\bar{y}_0^{(ts)}, \dots, \bar{y}_{T_s}^{(ts)}\}$ . To quantitatively evaluate the model performance, we introduce the FIT index, defined as

$$\text{FIT} = 100 \left( 1 - \frac{\sum_{k=0}^{T_s} \|\mathbf{y}_k^{(ts)} - \bar{\mathbf{y}}_k^{(ts)}\|_2}{\sum_{k=0}^{T_s} \|\bar{\mathbf{y}}_k^{(ts)} - \bar{\mathbf{y}}_{avg}\|_2} \right), \quad (31)$$

where  $\bar{\mathbf{y}}_{avg}$  is the average over sequence  $\bar{\mathbf{y}}^{(ts)}$ .

The trained Neural NARX model has scored 92.8% FIT index, which achieves satisfactory modeling performance.

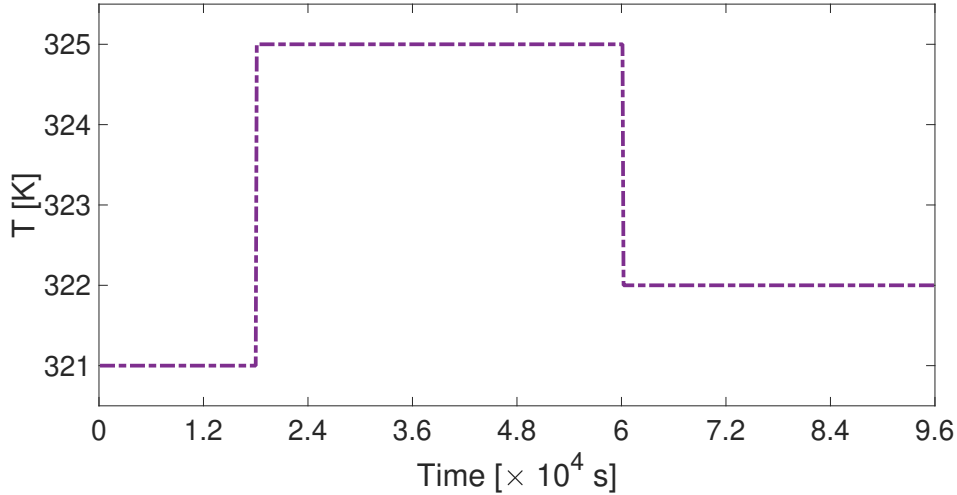


**Figure 5** Piecewise-constant output reference trajectory.

### 4.3 | Control synthesis

Now we are ready to implement the control framework in Section 3.

#### *Nominal MPC*

Let us first consider the offset-free tracking scheme proposed in 3.3, where model-plant mismatch is not considered in the MPC design. Our goal is to track piecewise constant water temperature references. The tracking reference is depicted in Figure 5. The nominal values of system parameters are reported in Table 1. The hyperparameters for MPC algorithm are reported in Table 2.  $Q_\theta$  is chosen much smaller than  $Q_x$  and  $Q_\xi$  to prioritize the tracking performance of MPC. And  $R = \text{diag}(R_e, R_u)$ . Integral gain  $\mu = 0.14$  is selected according to Proposition 2.

It should be noted that, for every new reference point  $y^o$  in Figure 5, the associated equilibrium point  $(\bar{x}(y^o), \bar{u}(y^o))$  should be computed again by solving (15), together with the target value for the augmented system  $(\bar{x}(y^o), \bar{v}(y^o), \bar{\zeta}(y^o))$ . The feasible output reference point is in the range

$$y^o \in (306.6, 337.2). \quad (32)$$

#### *Robust MPC*

Now let us consider the robust control scheme in 3.4. The first step is to estimate the upper bound of the model-plant mismatch  $\check{w}$  in (13). In the spirit of data-driven control approach, in this paper we estimate the upper bound from simulation data. The model (6) and the plant are simulated using 30 random reference trajectories, featuring different feasible setpoints, where 30 model output sequences  $\{\eta_1, \eta_2, \dots, \eta_{30}\}$  and real plant output sequences  $\{\bar{\eta}_1, \bar{\eta}_2, \dots, \bar{\eta}_{30}\}$  are obtained respectively. The  $\check{w}$  is estimated as the maximum error in the simulation data, i.e.,

$$\check{w} = \max_{i=1,2,\dots,30} \|\eta_i - \bar{\eta}_i\|_\infty \quad (33)$$

We obtain  $\check{w} = 0.031$ . The set  $\Omega_x$  is calculated using the estimated upper bound (33) and (26).

#### *Comparison and Discussion*

The popular offset-free control scheme in Reference 15 is implemented for comparison. The strategy, which is called Disturbance Estimation Based MPC (DEB-MPC), augments NNARX with a fictitious matched disturbance on the output. The disturbance model is estimated by a Moving Horizon Estimator (MHE). The hyperparameters for DEB-MPC are chosen in line with the proposed approach for a fair comparison.

The closed-loop tracking performances of the proposed nominal and robust approaches, together with DEB-MPC approach are reported in Fig 6. Although the DEB-MPC approach achieves better performance during the transient period, it fails to maintain zero tracking error due to the wrong disturbance model. Both proposed approaches attain asymptotic zero-error even in the presence of model-plant mismatch. The input of all schemes are reported in Figure 7. The constraints are satisfied in all cases. In addition, the robust approach requires less radical control effort compared to the other two approaches thanks to the tube design.

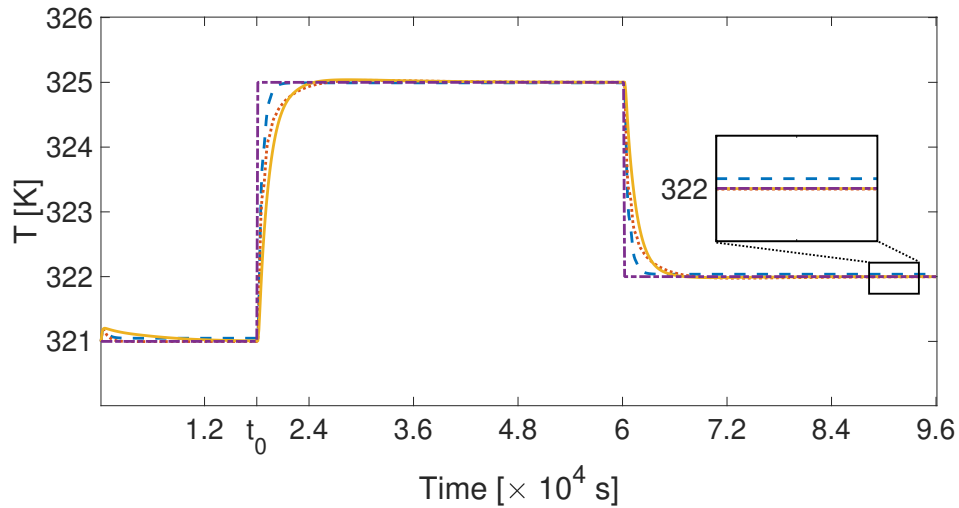


**Figure 6** Closed-loop output tracking performances of the proposed nominal approach (red dotted line), proposed robust approach (yellow continuous line) compared to that of the DEB-MPC (blue dashed line). The reference is represented by the purple dashed-dotted line.

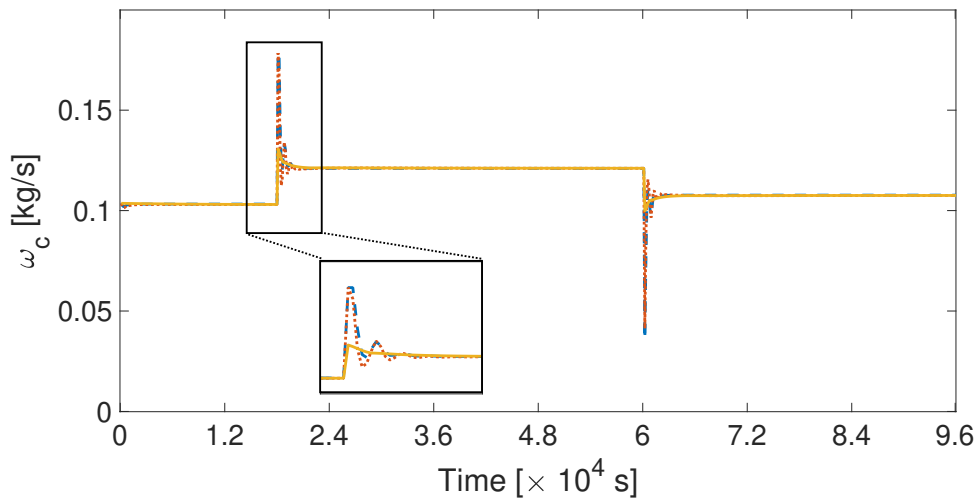


**Figure 7** Control input of the proposed nominal approach (red dotted line), proposed robust approach (yellow continuous line) compared to that of the DEB-MPC (blue dashed line).

In order to show the effectiveness of the tube design, the closed-loop output trajectory starting from  $t_0 = 1.8 \times 10^4 s$  is shown in Figure 8.  $t_0$  denotes the time when setpoint reference changes from 321 K to 325 K, see Figure 6. The nominal output trajectory predicted at  $t_0$  using the optimization in (27) is also shown with prediction horizon  $N = 50$ . It is clear that the real plant output is always contained within the tube  $\Omega_y$ , around the nominal output in the presence of model-plant mismatch.

Notably, the error bound in (33) is rather conservative since the maximum error occurs at the time instant where tracking setpoints change. During steady-state, however, the model-plant mismatch is in general much smaller. To this end, Reference 26 proposes a time-varying tube computed online to balance the trade-off between conservativeness and execution efficiency, which can be adopted in possible future works.

**Table 2** Hyperparameters for MPC algorithm

| Parameter | Adopted Value | Parameter  | Adopted Value                |
|-----------|---------------|------------|------------------------------|
| $N_p$     | 50            | $Q_x$      | $\text{diag}(R, R, R, R, R)$ |
| $R_e$     | 10            | $Q_\xi$    | 1                            |
| $R_u$     | 0.1           | $Q_\theta$ | $10^{-5}$                    |

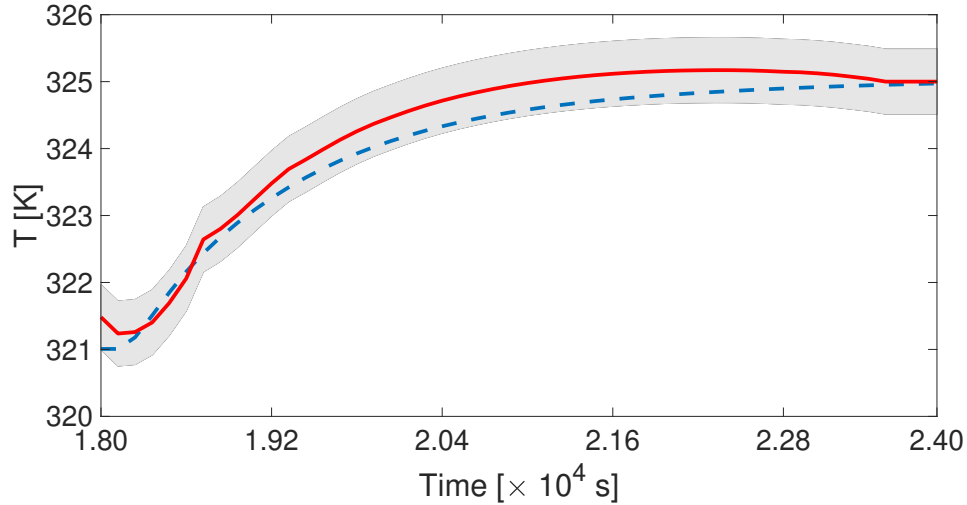


**Figure 8** Closed-loop output trajectory of robust approach (blue dashed line) compared to the open-loop nominal output trajectory (red continuous line) predicted at time  $t_0$ . The shaded area is the tube around the nominal trajectory.

## 5 | CONCLUSIONS

In this paper, a nonlinear robust Model Predictive Control (MPC) scheme is proposed for system learned by Neural NARX models. The model has been augmented with two additional elements, the integral action on the output tracking error and the derivative action on the MPC control variable. Moreover, based on the structure of Neural NARX model, a robust invariant set is designed. The resulting tube-based MPC keeps the real state within the prescribed tube around the nominal state. The proposed control scheme attains robust closed-loop stability and offset-free tracking abilities. Finally, the proposed control scheme is illustrated by a water heating benchmark system.

## ACKNOWLEDGEMENTS



This project has received funding from the European Union's Horizon 2020 research and innovation programme under the Marie Skłodowska-Curie grant agreement No. 953348

## References

1. Hou ZS, Wang Z. From model-based control to data-driven control: Survey, classification and perspective. *Information Sciences* 2013; 235: 3–35.
2. Schoukens J, Ljung L. Nonlinear system identification: A user-oriented road map. *IEEE Control Systems Magazine* 2019; 39(6): 28–99.
3. Hewing L, Kabzan J, Zeilinger MN. Cautious model predictive control using Gaussian process regression. *IEEE Transactions on Control Systems Technology* 2019; 28(6): 2736–2743.
4. Terzi E, Fagiano L, Farina M, Scattolini R. Learning-based predictive control for linear systems: A unitary approach. *Automatica* 2019; 108: 108473.
5. Green P, Cross E, Worden K. Bayesian system identification of dynamical systems using highly informative training data. *Mechanical Systems and Signal Processing* 2015; 56–57: 109–122. <https://doi.org/10.1098/rspa.1937.0036>.
6. Delgado A, Kambhampati C, Warwick K. Dynamic recurrent neural network for system identification and control. *IEE Proceedings-Control Theory and Applications* 1995; 142(4): 307–314.
7. Miller WT, Sutton RS, Werbos PJ. *Neural networks for control*. MIT press . 1995.
8. Bonassi F, Farina M, Scattolini R. On the stability properties of gated recurrent units neural networks. *Systems & Control Letters* 2021; 157: 105049.
9. Terzi E, Bonassi F, Farina M, Scattolini R. Learning model predictive control with long short-term memory networks. *International Journal of Robust and Nonlinear Control* 2021; 31(18): 8877–8896.
10. Armenio LB, Terzi E, Farina M, Scattolini R. Model predictive control design for dynamical systems learned by echo state networks. *IEEE Control Systems Letters* 2019; 3(4): 1044–1049.
11. Bonassi F, Farina M, Scattolini R. Stability of discrete-time feed-forward neural networks in NARX configuration. *IFAC-PapersOnLine* 2021; 54(7): 547–552.
12. Bonassi F, Farina M, Xie J, Scattolini R. On Recurrent Neural Networks for learning-based control: recent results and ideas for future developments. *Journal of Process Control* 2022; 114: 92–104.
13. Magni L, De Nicolao G, Scattolini R. Output feedback and tracking of nonlinear systems with model predictive control. *Automatica* 2001; 37(10): 1601–1607.
14. Bonassi F, Fabio C, Silva dO, Scattolini R. Nonlinear MPC for Offset-Free Tracking of systems learned by GRU Neural Networks. *IFAC-PapersOnLine* 2021; 54(14): 54–59.
15. Morari M, Maeder U. Nonlinear offset-free model predictive control. *Automatica* 2012; 48(9): 2059–2067.
16. Scokaert PO, Mayne DQ. Min-max feedback model predictive control for constrained linear systems. *IEEE Transactions on Automatic control* 1998; 43(8): 1136–1142.
17. Mayne DQ, Seron MM, Raković S. Robust model predictive control of constrained linear systems with bounded disturbances. *Automatica* 2005; 41(2): 219–224.
18. Langson W, Chrysoschoos I, Raković S, Mayne DQ. Robust model predictive control using tubes. *Automatica* 2004; 40(1): 125–133.
19. Bonassi F, Xie J, Farina M, Scattolini R. An Offset-Free Nonlinear MPC scheme for systems learned by Neural NARX models. *arXiv preprint arXiv:2203.16290* 2022.
20. De Nicolao G, Magni L, Scattolini R. Stabilizing predictive control of nonlinear ARX models. *Automatica* 1997; 33(9): 1691–1697.

21. Francis BA, Wonham WM. The internal model principle of control theory. *Automatica* 1976; 12(5): 457–465.
22. Scattolini R, Schiavoni N. A parameter optimization approach to the design of structurally constrained regulators for discrete-time systems. *International Journal of Control* 1985; 42(1): 177–192.
23. Rawlings JB, Mayne DQ, Diehl M. *Model predictive control: theory, computation, and design*. 2. Nob Hill Publishing Madison, WI . 2017.
24. Kolmanovsky I, Gilbert EG. Theory and computation of disturbance invariant sets for discrete-time linear systems. *Mathematical problems in engineering* 1998; 4(4): 317–367.
25. Jaeger H. Tutorial on training recurrent neural networks, covering BPPT, RTRL, EKF and the "echo state network" approach. 2002.
26. Gonzalez R, Fiacchini M, Alamo T, Guzmán JL, Rodríguez F. Online robust tube-based MPC for time-varying systems: A practical approach. *International Journal of Control* 2011; 84(6): 1157–1170.
27. Khalil HK. *Nonlinear systems; 3rd ed*. Prentice-Hall . 2002.
28. Bof N, Carli R, Schenato L. Lyapunov theory for discrete time systems. *arXiv preprint arXiv:1809.05289* 2018.



## APPENDIX

### A PROOFS

#### A.1 Proof of Proposition 1

*Proof.* Let  $\delta x_k$  and  $\delta u_k$  be the displacement from the equilibrium point  $(\bar{x}, \bar{u})$ , i.e.  $x_k = \bar{x} + \delta x_k$  and  $u_k = \bar{u} + \delta u_k$ . The nonlinear system (9) can be rewritten as

$$\delta x_{k+1} + \bar{x} = f(\bar{x} + \delta x_k, \bar{u} + \delta u_k). \quad (\text{A1})$$

Since the goal is to analyze the asymptotic stability of the linearized system, for simplicity it is assumed that  $\delta u_k = 0$ . It is worth noticing, however, that this proof could be easily extended to consider  $\delta u_k \neq 0$ , at the price of more involved computations. Under this simplification, (A2) reads

$$\delta x_{k+1} + \bar{x} = f(\bar{x} + \delta x_k, \bar{u}). \quad (\text{A2})$$

System (A2) can be recast as its linearization plus the linearization error  $\varepsilon$

$$\delta x_{k+1} = A_\delta \delta x_k + \varepsilon(\delta x_k), \quad (\text{A3})$$

where

$$A_\delta = \left. \frac{\partial f}{\partial x} \right|_{\bar{x}, \bar{u}}. \quad (\text{A4})$$

The goal is to show that the linear system

$$\delta x_{k+1} = A_\delta \delta x_k \quad (\text{A5})$$

is asymptotically stable. Along the lines of Reference 27, the linearization error is first bounded as follows.

Consider the  $i$ -th state component, with  $i \in \{1, \dots, n\}$ . In light of the Mean Value Theorem there exists  $\tilde{x}$  between  $\bar{x}$  and  $\bar{x} + \delta x_k$  such that

$$\begin{aligned} f_i(\bar{x} + \delta x_k, \bar{u}) - f_i(\bar{x}, \bar{u}) &= \left. \frac{\partial f_i(x, \bar{u})}{\partial x} \right|_{\tilde{x}, \bar{u}} \delta x_k \\ &= \left. \frac{\partial f_i(x, \bar{u})}{\partial x} \right|_{\bar{x}, \bar{u}} \delta x_k + \left[ \left. \frac{\partial f_i(x, \bar{u})}{\partial x} \right|_{\tilde{x}, \bar{u}} - \left. \frac{\partial f_i(x, \bar{u})}{\partial x} \right|_{\bar{x}, \bar{u}} \right] \delta x_k \\ &= A_{\delta_i} \delta x_k + \tilde{\varepsilon}_i(\delta x_k) \delta x_k \end{aligned} \quad (\text{A6})$$

In the light of the assumption on the Lipschitz continuity of the gradient of  $f(x, \bar{u})$ , it holds that

$$\begin{aligned} \|\tilde{\varepsilon}_i(\delta x_k)\|_2^2 &\leq \left\| \frac{\partial f_i(x, \bar{u})}{\partial x} \Big|_{\bar{x}, \bar{u}} - \frac{\partial f_i(x, \bar{u})}{\partial x} \Big|_{\bar{x}, \bar{u}} \right\|_2^2 \\ &\leq L_1^2 \|\bar{x} - \bar{x}\|_2^2 \leq L_1^2 \|\delta x_k\|_2^2. \end{aligned} \quad (\text{A7})$$

Hence, being  $\varepsilon(\delta x_k) = \tilde{\varepsilon}(\delta x_k)\delta x_k$ , the linearization error can be bounded as

$$\begin{aligned} \|\varepsilon(\delta x_k)\|_2 &\leq \|\delta x_k\|_2 \sqrt{\sum_{i=1}^n \|\tilde{\varepsilon}_i(\delta x_k)\|_2^2} \|\delta x_k\|_2 \\ &\leq L_\varepsilon \|\delta x_k\|_2^2, \end{aligned} \quad (\text{A8})$$

where  $L_\varepsilon = L_1 \sqrt{n}$ .

At this stage, let us recall that the  $\delta$ ISS property implies the Global Asymptotic Stability (GAS) of any equilibrium. Indeed, recalling that  $\delta u_k = 0$ , from (10) it follows that

$$\|x_k - \bar{x}\|_2 \leq \beta(\|x_0 - \bar{x}\|_2, k).$$

Moreover, in light of the assumption on  $\beta$ , the exponential GAS property of any equilibrium can be shown, since

$$\|\delta x_k\|_2 \leq \rho \|\delta x_0\|_2 \lambda^k. \quad (\text{A9})$$

This allows to invoke Theorem 5.8 in Reference 28, which, under the assumption of exponential GAS, guarantees the existence of a quadratic Lyapunov function  $V(\delta x)$  for the nonlinear system (A2). That is, there exist positive constants  $c_1, c_2, c_3, c_4$ , such that

$$c_1 \|\delta x_k\|_2^2 \leq V(\delta x_k) \leq c_2 \|\delta x_k\|_2^2, \quad (\text{A10a})$$

$$V(A_\delta \delta x_k + \varepsilon(\delta x_k)) - V(\delta x_k) \leq -c_3 \|\delta x_k\|_2^2 \quad (\text{A10b})$$

$$\left\| \frac{\partial V(A_\delta \delta x_k + \varepsilon(\delta x_k))}{\partial \varepsilon} \right\|_2 \leq c_4 \|\delta x_k\|_2. \quad (\text{A10c})$$

The goal is to show that  $V(\delta x_k)$  is also a Lyapunov function for the linear system (A5). To this end, let us add and subtract  $V(A_\delta \delta x_k)$  from the left-hand side of (A10b), leading to

$$\begin{aligned} V(A_\delta \delta x_k) - V(\delta x_k) + [V(A_\delta \delta x_k + \varepsilon(\delta x_k)) - V(A_\delta \delta x_k)] \\ \leq -c_3 \|\delta x_k\|_2^2 \end{aligned} \quad (\text{A11})$$

In light of (A10c) and (A8),  $V(A_\delta \delta x_k + \varepsilon(\delta x_k)) - V(A_\delta \delta x_k)$  can be bounded as

$$\begin{aligned} \left\| V(A_\delta \delta x_k + \varepsilon(\delta x_k)) - V(A_\delta \delta x_k) \right\|_2 \\ \leq \left\| \frac{\partial V(A_\delta \delta x_k + \varepsilon(\delta x_k))}{\partial \varepsilon} \right\|_2 \|\delta x_k\|_2 \\ \leq c_4 L_\varepsilon \|\delta x_k\|_2^3. \end{aligned} \quad (\text{A12})$$

Owing to the bound (A12) and to the exponential GAS (A9), recalling that  $\lambda \in (0, 1)$ , from (A11) it holds that

$$\begin{aligned} V(A_\delta \delta x_k) - V(\delta x_k) &\leq -c_3 \|\delta x_k\|_2^2 - c_4 L_\varepsilon \|\delta x_k\|_2^3 \\ &\leq -c_3 \|\delta x_k\|_2^2 - \rho c_4 L_\varepsilon \|\delta x_0\|_2 \|\delta x_k\|_2^2 \\ &\leq -(c_3 - \rho c_4 L_\varepsilon \|\delta x_0\|_2) \|\delta x_k\|_2^2. \end{aligned} \quad (\text{A13})$$

Hence, there exist constants  $c_5 > 0$  and  $r_0 > 0$  such that,  $\forall \delta x_0 \in \{\delta x_0 : \|\delta x_0\|_2 \leq r_0\}$ ,

$$V(A_\delta \delta x_k) - V(\delta x_k) \leq -c_5 \|\delta x_k\|_2^2.$$

The asymptotic stability of the linear system (A5) is proven by using  $V(\delta x_k)$  as Lyapunov function, which implies that  $A_\delta$  is Schur stable. □